Supporting Information

Separation of 300 and 100 nm Particles in Fabry–Perot Acoustofluidic Resonators

Prateek Sehgal[†] and Brian J. Kirby[†‡*]

[†]Sibley School of Mechanical and Aerospace Engineering, Cornell University, Ithaca, New York 14853, USA.

[‡] Department of Medicine, Division of Hematology & Medical Oncology, Weill–Cornell Medicine, New York, New York 10021, USA.

*Corresponding author – Email: kirby@cornell.edu , Tel.: (+1)607-255-4379

Analytical model for particle transport: Derivations

Decomposing the mobility tensor in eq 2 into M_{xy} and M_z component, assuming the fields are x-independent, and considering the Stokes–Einstein relation for diffusivity $\bar{\bar{D}} = k_B T \bar{\bar{M}}$, the steady-state governing equation can be written as

$$0 = \frac{\partial}{\partial y}\left(u_y P_o^\infty - M_{xy}\frac{\partial V_a}{\partial y} P_o^\infty - k_B T M_{xy}\frac{\partial P_o^\infty}{\partial y}\right) + \frac{\partial}{\partial z}\left(-M_z\frac{\partial V_a}{\partial z} P_o^\infty - k_B T M_z\frac{\partial P_o^\infty}{\partial z}\right) \quad \text{(S1)}$$

where k_B is the Boltzmann constant and T is the absolute temperature. The variables in the governing equation are nondimensionalized with the following scheme –

$$\begin{aligned} x^* &= x / l_x \\ y^* &= y / \Lambda \\ z^* &= z / h \\ u_y^* &= u_y / U_{Fy} \\ P_o^{\infty *} &= \mathrm{V} P_o^\infty \\ M_{xy/z}^* &= M_{xy/z} / M_\infty \\ V_a^* &= V_a / k_B T \end{aligned} \quad \text{(S2)}$$

where M_∞ is the bulk mobility and U_{Fy} is the y-component of the external flow field $\mathrm{U_F}$. The superscript star is dropped from the nondimensionalized variables with the understanding that the mentioned variables are nondimensionalized hereafter, unless stated otherwise.

Following the Fick-Jacobs approximation,[1,2] the conditional probability density P_o^∞ can be written in terms of marginal probability density $P_m(y)$ as –

$$P_o^\infty = \frac{P_m(y)}{I(y)} e^{-V_a} \quad \text{(S3)}$$

where $I(y) = \iint e^{-V_a}\, dxdz$. Upon substitution of eq S3, eq S1 can be solved with the conditions described in eq 3 to yield a closed-form analytical solution of $P_m(y)$ and, consequently, P_o^∞ –

$$P_m(y) = e^{\mathrm{Pe}\phi(y)} \frac{\left(-\left(1 - e^{\mathrm{Pe}\phi(1)}\right)\int_0^y k(y')dy' + \int_0^1 k(y')dy' \right)}{\int_0^1 I(y) e^{\mathrm{Pe}\phi(y)} \left(\int_y^{y+1} k(y')dy' \right) dy} I(y) \quad \text{(S4)}$$

$$P_o^\infty = e^{\mathrm{Pe}\phi(y) - V_a} \frac{\left(-\left(1 - e^{\mathrm{Pe}\phi(1)}\right)\int_0^y k(y')dy' + \int_0^1 k(y')dy' \right)}{\int_0^1 I(y) e^{\mathrm{Pe}\phi(y)} \left(\int_y^{y+1} k(y')dy' \right) dy} \quad \text{(S5)}$$

with $k(y')$ being defined as –

$$k(y') = \frac{1}{e^{\mathrm{Pe}\phi(y')} I(y') \bar{M}_{xy}(y')} \quad \text{(S6)}$$

where Pe is the Peclet number defined as $\mathrm{Pe} = U_{Fy}\Lambda / k_B T M_\infty$, $\phi(y) = \bar{u}_y / \bar{M}_{xy}(y)$ is the local effective hydrodynamic force, and $\bar{M}_{xy} = \iint M_{xy} e^{-V_a}\, dxdz \Big/ I(y)$ and $\bar{u}_y = \iint u_y e^{-V_a}\, dxdz \Big/ I(y)$ are the local average of mobility and velocity, respectively.

To obtain the particle trajectories from eq S5, the flux of the probability density in x- and y-directions are integrated to yield the average migration velocity of the particle as following –

$$U_{px} = \iiint u_x P_o^{\infty} dxdydz$$

$$U_{py} = \frac{M_\infty k_B T}{\Lambda} \iiint_1 \frac{1 - e^{-\mathrm{Pe}\phi(1)}}{\int_0 I(y) e^{\mathrm{Pe}\phi(y)} \left(\int_y^{y+1} k(y')dy' \right) dy} dxdydz \quad \text{(S7)}$$

Here U_{px}, U_{py}, and u_x are dimensional variables whereas other variables are nondimensional as stated previously. Finally, the migration angle θ of a particle is calculated by $\tan\theta = U_{px}/U_{py}$.

The acoustic potential (V_a) is obtained from the 2D

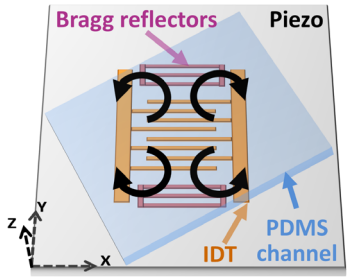

Figure S1. Schematic of the device illustrating the acoustic streaming vortices observed in no external-flow condition. The black arrows show the vortices and the direction of the streaming flow.

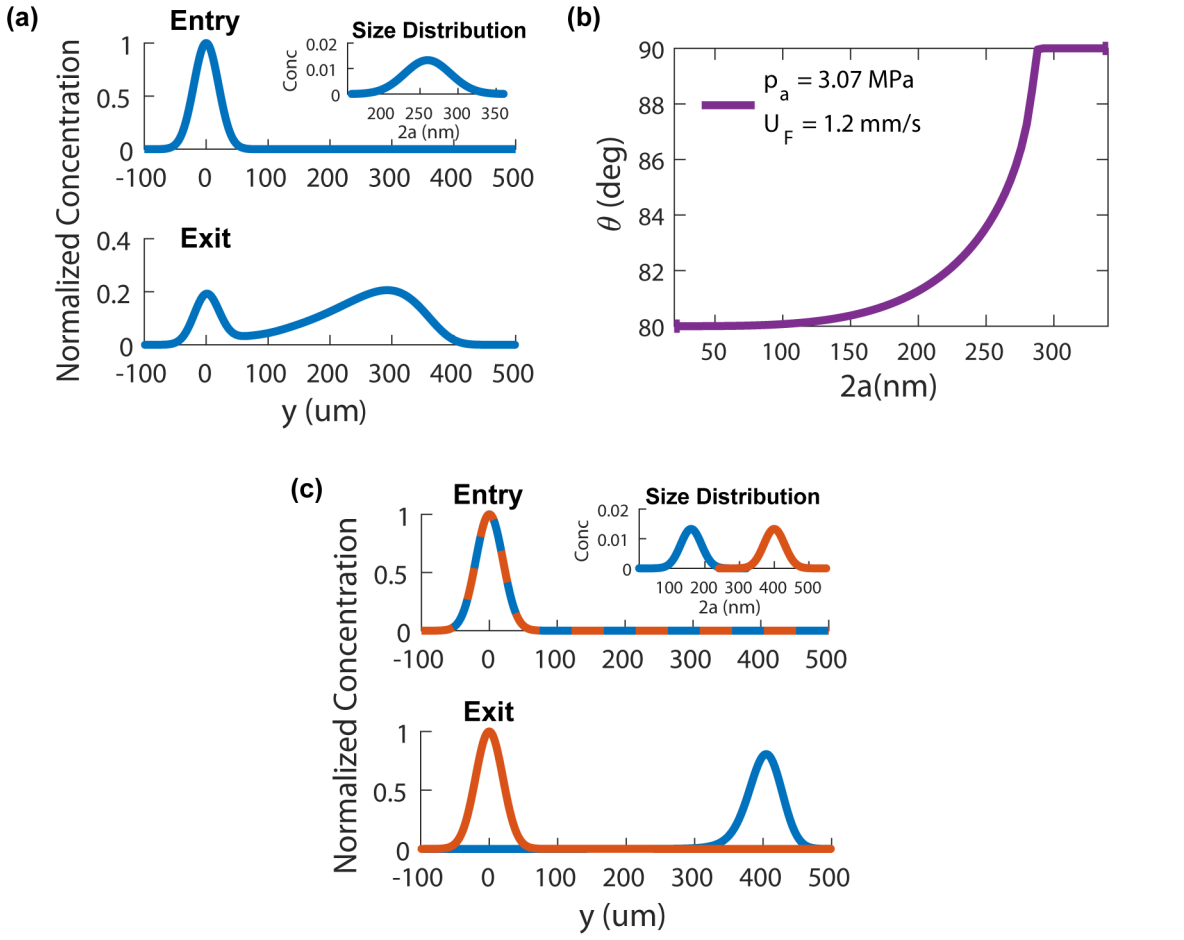

Figure S2. Transport of heterogeneous populations of submicron particles in the Fabry-Perot acoustofluidic device. The populations are considered normally distributed in the y direction (mean=0, standard deviation = 20 um) at the entry of the IDT, as shown by the Entry plot. The normalized concentration distribution at entry is transported over the IDT region based on our analytical model to obtain the population distribution at the exit of the IDT, as shown by the Exit plot. (a) Shows the migration of a widely distributed polystyrene population at the experimental conditions of power density 0.12 w/mm^2 and flow rate 12.2 ul/min (i.e. p_a = 3.07 MPa , U_F = 1.2 mm/s). The threshold diameter is 290 nm. The inset shows the normal size distribution of the particles with mean and standard deviation 260 nm and 30 nm, respectively. (b) Shows the variation of migration angle with size for polystyrene particles, which is used to sample the migration angle for each particle size in (a). (c) Shows the separation of subpopulations of extracellular vesicles at power density 0.162 W/mm^2 and flow rate 12.2 ul/min (i.e. p_a = 3.57 MPa , U_F = 1.2 mm/s). The threshold diameter is 300 nm. The inset shows the normal size distribution of the microvesicles (orange) and the exosomes (blue) with the means 400 nm and 160 nm, respectively, and the standard deviation 30 nm for both subpopulations.

frequency-domain finite element simulations of the system in COMSOL Multiphysics 4.3. We have solved constitutive equations for piezoelectric substrates[3] to obtain SAW displacement field in 80 um (λ) wide and 200 um thick 128° Y-X cut lithium niobate domain. One finger-pair of the IDT is simulated with periodic boundary conditions for displacement and electric potential at y-boundaries. The width of each electrode and the spacing between electrodes is 20 um. The displacement field in lithium niobate is coupled to the fluid domain of height 50 um and serves as the boundary condition at z=0 boundary of the fluid domain. Pressure field in the fluid is obtained by solving Helmholtz wave equation with periodic boundary condition in pressure at y-boundaries. Impedance boundary condition, corresponding to the acoustic impedance of PDMS, is applied at the top channel wall to model fluid-PDMS interface. Frequency sweep from 48 MHz to 49.5 MHz estimated the resonance frequency at 48.9 MHz, which is in close agreement with the experimental value of 48.8 MHz for particle separation studies.

Acoustic streaming

In the no external-flow condition, we observe four counter-rotating streaming vortices as shown in Figure S1. These vortices result in a stagnation point approximately at the center of the IDT. Because of the no flux boundary condition normal to the channel wall, the vortices field is determined by the relative orientation of the PDMS to the IDT and, therefore, depends on θ_f. This streaming field perturbs the external flow field. However, as evident from the particle bands in Figure 5a, the streaming field does not significantly influence the acoustophoresis of 300 nm particles in our device.

Transport of heterogeneous populations of particles

Here, we investigate with our analytical model the transport of heterogeneous populations of particle in the Fabry-Perot acoustofluidic system. Figure S2a shows the migration of a widely distributed population of polystyrene particles at same experimental conditions as that in Figure 5a. We obtain these results by sampling the migration angle from the theta–size curve shown in Figure S2b that is calculated for experimentally estimated pressure amplitude and average velocity. The final distribution of the particles (Exit) is obtained from the initial distribution (Entry) by transporting each particle within the size distribution (inset) by its corresponding sampled migration angle. A peak at y=0 in the exit plot corresponds to the particles that are larger than the threshold diameter and undergo no y displacement.

Because our analytical model can estimate the transport of any heterogeneous population, we then turn to analytically investigate the separation of heterogeneous biological nanoparticles. Particularly, we apply our analytical model in conjunction with our experimental measurements to estimate the transport and separation of heterogeneous subpopulations of extracellular vesicles, i.e. microvesicles and exosomes, in the Fabry-Perot device. Inset of Figure S2c shows the considered size-distribution of microvesicles and exosomes based on the distribution reported by Lee *et al.*[4] in their study on acoustic separation of these subpopulations. To separate these subpopulations of vesicles, a suitable choice of the threshold diameter is 300 nm.[4] Because the vesicles have different acoustic properties than the polystyrene particles, the external power must be tuned appropriately, at fixed flow rate, to set the desired threshold diameter. From our previous estimation of the pressure amplitude and the understanding that the applied power scales with the square of the pressure amplitude,[5] we estimate that it requires 35% more power density than that in Figure 5a to set the threshold diameter to 300 nm for vesicles and separate the subpopulations. Figure S2c shows our analytical prediction for the transport of vesicles in the Fabry-Perot device and demonstrates the separation of two subpopulations of vesicles.

REFERENCES

(1) Bernate, J. A.; Drazer, G. *J. Colloid Interface Sci.* **2011**, *356* (1), 341–351.
(2) Zwanzig, R. *J. Phys. Chem.* **1992**, *96 (10)*, 3926–3930.
(3) Tiersten, H. F. *J Acoust. Soc. Am.* **1963**, 35 (2), 234–239.
(4) Lee, K.; Shao, H.; Weissleder, R.; Lee, H. *ACS Nano* **2015**, *9* (3), 2321–2327.
(5) Barnkob, R.; Augustsson, P.; Laurell, T.; Bruus, H. *Lab Chip* **2010**, *10* (5), 563–570.